Chapter 2
Mathematical Modeling of Convective Heat Transfer in Rotating-Disk Systems

2.1 Differential and Integral Equations

2.1.1 Navier–Stokes and Energy Equations in Differential Form

A schematic of a stationary axisymmetric problem of convective heat transfer over rotating disks, whose axis of symmetry serves as the axis z of a stationary cylindrical coordinate system with the point $z = 0$ placed on the disk surface, is depicted in Fig. 2.1. The angular velocity is high, so that gravitational effects are negligible, i.e., $F_r = F_\varphi = F_z = 0$.

Thus, Eqs. (1.21)–(1.25) are reduced [1–3] to

$$v_r\frac{\partial v_r}{\partial r}+v_z\frac{\partial v_r}{\partial z}-\frac{v_\varphi^2}{r}=-\frac{1}{\rho}\frac{\partial p}{\partial r}+\nu\left(\nabla^2 v_r-\frac{v_r}{r^2}\right)-\left[\frac{1}{r}\frac{\partial}{\partial r}\left(r\overline{v_r'^2}\right)+\frac{\partial}{\partial z}\left(\rho\overline{v_r'v_z'}\right)-\frac{1}{r}\left(\overline{v_\varphi'^2}\right)\right], \tag{2.1}$$

$$v_r\frac{\partial v_\varphi}{\partial r}+\frac{v_r v_\varphi}{r}+v_z\frac{\partial v_\varphi}{\partial z}=\nu\left(\frac{\partial^2 v_\varphi}{\partial r^2}+\frac{1}{r}\frac{\partial v_\varphi}{\partial r}-\frac{v_\varphi}{r^2}+\frac{\partial^2 v_\varphi}{\partial z^2}\right)-\left[\frac{1}{r^2}\frac{\partial}{\partial r}\left(r^2\overline{v_r'v_\varphi'}\right)+\frac{\partial}{\partial z}\left(\overline{v_\varphi'v_z'}\right)\right], \tag{2.2}$$

$$v_r\frac{\partial v_z}{\partial r}+v_z\frac{\partial v_z}{\partial z}=-\frac{1}{\rho}\frac{\partial p}{\partial z}+\nu\left(\frac{\partial^2 v_z}{\partial r^2}+\frac{1}{r}\frac{\partial v_z}{\partial r}+\frac{\partial^2 v_z}{\partial z^2}\right)-\left[\frac{1}{r}\frac{\partial}{\partial r}\left(r\overline{v_r'v_z'}\right)+\frac{\partial}{\partial z}\left(\overline{v_z'^2}\right)\right], \tag{2.3}$$

I.V. Shevchuk, *Modelling of Convective Heat and Mass Transfer in Rotating Flows*, Mathematical Engineering, DOI 10.1007/978-3-319-20961-6_2

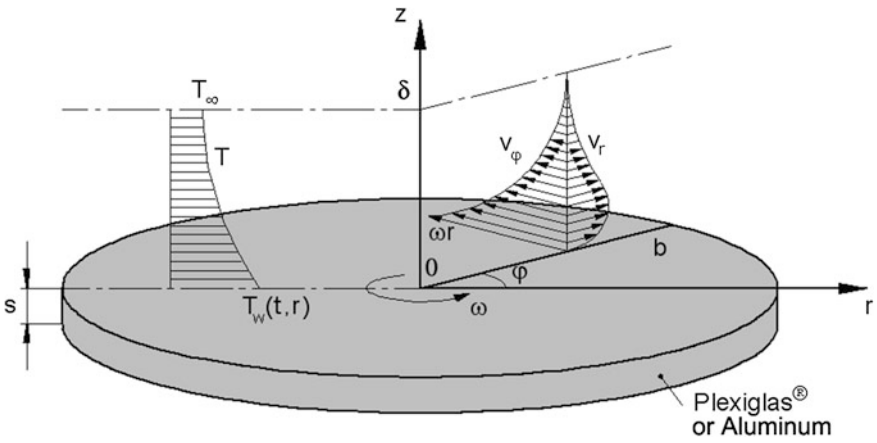

Fig. 2.1 Geometrical arrangement and main parameters of the problem of fluid flow and heat transfer over a rotating disk in still air [3]

$$\frac{\partial v_r}{\partial r} + \frac{v_r}{r} + \frac{\partial v_z}{\partial z} = 0, \tag{2.4}$$

$$\frac{\partial T}{\partial t} + v_r \frac{\partial T}{\partial r} + v_z \frac{\partial T}{\partial z} = \frac{1}{r}\frac{\partial}{\partial r}\left[r\left(a\frac{\partial T}{\partial r} - \overline{v_r' T'}\right)\right] + \frac{\partial}{\partial z}\left(a\frac{\partial T}{\partial z} - \overline{v_z' T'}\right). \tag{2.5}$$

One can assign the coordinate system in Fig. 2.1 to be rotating together with the disk. In doing so, Eqs. (2.1)–(2.3) for laminar flow can be re-written as [1–3]

$$v_r \frac{\partial v_r}{\partial r} + v_z \frac{\partial v_r}{\partial z} - \frac{v_\varphi^2}{r} - 2\omega v_\varphi - \omega^2 r = -\frac{1}{\rho}\frac{\partial p}{\partial r} + \nu\left(\frac{\partial^2 v_r}{\partial r^2} + \frac{1}{r}\frac{\partial v_r}{\partial r} - \frac{v_r}{r^2} + \frac{\partial^2 v_r}{\partial z^2}\right), \tag{2.6}$$

$$v_r \frac{\partial v_\varphi}{\partial r} + v_z \frac{\partial v_\varphi}{\partial z} + \frac{v_r v_\varphi}{r} + 2\omega v_r = \nu\left(\frac{\partial^2 v_\varphi}{\partial r^2} + \frac{1}{r}\frac{\partial v_\varphi}{\partial r} - \frac{v_\varphi}{r^2} + \frac{\partial^2 v_\varphi}{\partial z^2}\right), \tag{2.7}$$

$$v_r \frac{\partial v_z}{\partial r} + v_z \frac{\partial v_z}{\partial z} = -\frac{1}{\rho}\frac{\partial p}{\partial z} + \nu\left(\frac{\partial^2 v_z}{\partial r^2} + \frac{1}{r}\frac{\partial v_z}{\partial r} + \frac{\partial^2 v_z}{\partial z^2}\right). \tag{2.8}$$

The terms $2\omega v_\varphi$ and $2\omega v_r$ stand for the r- and φ-components of the Coriolis force, respectively. The term $\omega^2 r$ is the r-component of the centrifugal force (all divided by ρ). Equations (2.1)–(2.2) for turbulent flow can be derived in analogy to Eqs. (2.6)–(2.8) [1].

2.1.2 Differential Equations of the Boundary Layer

To simplify Eqs. (2.1)–(2.5) for boundary layers, the following assumptions are made [1, 2, 4]:

(a) velocity components v_r and v_φ are an order of magnitude larger than the v_z-velocity;
(b) velocity and temperature vary in the z-direction much more significantly than they do in the r-direction; and
(c) variation of the static pressure in z-direction is negligible.

The equation of continuity, Eq. (2.4), does not undergo any change. As a result, Eqs. (2.1)–(2.5) reduce to the following final form [1, 2, 4]:

$$v_r \frac{\partial v_r}{\partial r} + v_z \frac{\partial v_r}{\partial z} - \frac{v_\varphi^2}{r} = -\frac{1}{\rho}\frac{\partial p}{\partial r} + \frac{1}{\rho}\frac{\partial \tau_r}{\partial z}, \tag{2.9}$$

$$v_r \frac{\partial v_\varphi}{\partial r} + v_z \frac{\partial v_\varphi}{\partial z} + \frac{v_r v_\varphi}{r} = \frac{1}{\rho}\frac{\partial \tau_\varphi}{\partial z}, \tag{2.10}$$

$$\frac{1}{\rho}\frac{\partial p}{\partial z} = 0, \tag{2.11}$$

$$\frac{\partial T}{\partial t} + v_r \frac{\partial T}{\partial r} + v_z \frac{\partial T}{\partial z} = -\frac{1}{\rho c_p}\frac{\partial q}{\partial z}, \tag{2.12}$$

$$\tau_r = \mu \frac{\partial v_r}{\partial z} - \rho \overline{v_r' v_z'}, \tag{2.13}$$

$$\tau_\varphi = \mu \frac{\partial v_\varphi}{\partial z} - \rho \overline{v_\varphi' v_z'}, \tag{2.14}$$

$$q = -\left(\lambda \frac{\partial T}{\partial z} - \rho c_p \overline{T' v_z'}\right). \tag{2.15}$$

The pressure across the boundary layer is constant and equal to the pressure in the potential flow region, i.e., $p = p_\infty$. Equations (2.13)–(2.15) include only the most significant turbulent shear stress and heat flux components.

For a stationary thermal boundary layer, the term $\partial T/\partial t$ in Eq. (2.12) vanishes.

Equations (2.9)–(2.15) are closed with an equation of potential flow, where functions $v_{r,\infty}$, $v_{\varphi,\infty}$, and p_∞ do not vary in the z-direction:

$$\frac{1}{2}\frac{\mathrm{d}v_{r,\infty}^2}{\mathrm{d}r} - \frac{v_{\varphi,\infty}^2}{r} = -\frac{1}{\rho}\frac{\mathrm{d}p_\infty}{\mathrm{d}r}. \tag{2.16}$$

2.1.3 Integral Equations of the Boundary Layer

For steady-state conditions, Eqs. (2.9)–(2.11), (2.13)–(2.20) with allowance for Eqs. (2.4) and (2.16) can be re-written in an integral form [1, 2, 4]:

$$\frac{\mathrm{d}}{\mathrm{d}r}\left[r\int_0^{\delta} v_r\left(v_{r,\infty}-v_r\right)\mathrm{d}z\right]+r\frac{\mathrm{d}v_{r,\infty}}{\mathrm{d}r}\int_0^{\delta}\left(v_{r,\infty}-v_r\right)\mathrm{d}z-\int_0^{\delta}\left(v_{\varphi,\infty}^2-v_{\varphi}^2\right)\mathrm{d}z = r\tau_{wr}/\rho, \tag{2.17}$$

$$\frac{\mathrm{d}}{\mathrm{d}r}\left[r^2\int_0^{\delta} v_r\left(v_{\varphi}-v_{\varphi,\infty}\right)\mathrm{d}z\right]+\frac{\dot{m}_d}{2\pi\rho}\frac{\mathrm{d}}{\mathrm{d}r}\left(rv_{\varphi,\infty}\right) = -r^2\tau_{w\varphi}/\rho, \tag{2.18}$$

or

$$\frac{\mathrm{d}}{\mathrm{d}r}\left[r^2\int_0^{\delta} v_r v_{\varphi}\mathrm{d}z\right]+rv_{\varphi,\infty}\frac{\mathrm{d}}{\mathrm{d}r}\left(\frac{\dot{m}_d}{2\pi\rho}\right) = -r^2\tau_{w\varphi}/\rho, \tag{2.19}$$

$$\frac{\mathrm{d}}{\mathrm{d}r}\left[r\int_0^{\delta_T} v_r(T-T_{\infty})\mathrm{d}z\right]+\frac{\mathrm{d}T_{\infty}}{\mathrm{d}r}\cdot\frac{\dot{m}_{d,T}}{2\pi\rho} = rq_w/(\rho c_p). \tag{2.20}$$

Another notation of Eqs. (2.17), (2.18) and (2.20) looks as [1, 2, 4, 5]

$$\frac{\mathrm{d}}{\mathrm{d}r}\left(v_{r,\infty}^2 r\delta\overline{\delta}_r^{**}\right)+v_{r,\infty}r\delta\frac{\mathrm{d}v_{r,\infty}}{\mathrm{d}r}\overline{\delta}_r^{*}-v_{\varphi,\infty}^2\delta\overline{\delta}_{\varphi}^{**} = r\tau_{wr}/\rho, \tag{2.21}$$

$$\frac{\mathrm{d}}{\mathrm{d}r}\left[\delta r^2(\omega r)^2\overline{\delta}_{\varphi r}^{**}\right]+\frac{\dot{m}_d}{2\pi\rho}\frac{\mathrm{d}}{\mathrm{d}r}(rv_{\varphi,\infty}) = -r^2\tau_{w\varphi}/\rho, \tag{2.22}$$

$$\frac{\mathrm{d}}{\mathrm{d}r}\left[\omega r^2\delta\overline{\delta}_T^{**}(T_w-T_{\infty})\right]+\frac{\mathrm{d}T_{\infty}}{\mathrm{d}r}\cdot\frac{\dot{m}_{d,T}}{2\pi\rho} = rq_w/(\rho c_p), \tag{2.23}$$

where

$$\overline{\delta}_r^{*}=\int_0^1(1-\tilde{v}_r)\mathrm{d}\xi,\quad \overline{\delta}_r^{**}=\int_0^1\tilde{v}_r(1-\tilde{v}_r)\mathrm{d}\xi,\quad \overline{\delta}_{\varphi}^{**}=\int_0^1\left(1-\frac{v_{\varphi}^2}{v_{\varphi,\infty}^2}\right)\mathrm{d}\xi, \tag{2.24}$$

$$\overline{\delta}_{\varphi r}^{**}=\int_0^1\frac{v_r(v_{\varphi}-v_{\varphi,\infty})}{(\omega r)^2}\mathrm{d}\xi,\quad \tilde{v}_r=v_r/v_{r,\infty}. \tag{2.25}$$

2.2 Methods of Solution

2.2.1 Self-similar Solution

Exact solutions of the Navier–Stokes and energy equations were found for a free rotating disk subject to laminar flow [1, 2, 4, 6–12]. For this purpose, self-similar variables F, G, H, P, and ζ were employed:

$$\begin{array}{lll} v_r = (a+\omega) r F(\zeta), & v_\varphi = (a+\omega) r G(\zeta), & v_z = \sqrt{(a+\omega)\nu} H(\zeta), \\ p = -\rho \nu \omega P(\zeta), & \theta = (T - T_\infty)/(T_w - T_\infty), & \zeta = z\sqrt{(a+\omega)/\nu}. \end{array} \tag{2.26}$$

The respective boundary conditions had the following form:

$$\zeta \to \infty: v_{r,\infty} = ar, \quad v_{z,\infty} = -2az, \quad v_{\varphi,\infty} = \Omega r, \quad \beta = \Omega/\omega = \text{const.}, \quad \theta = 0, \tag{2.27}$$

$$\zeta = 0: F = H = 0, \quad G = 1, \quad \theta = 1, \tag{2.28}$$

$$\zeta = 0: T_w = T_{\text{ref}} + c_{0w} r^{n_*}, \quad T_\infty = T_{\text{ref}} + c_{0\infty} r^{n_*} \text{ or } T_\infty = T_{\text{ref}} + \beta c_{0w} r^{n_*}. \tag{2.29}$$

Here, c_0, c_{0w}, $c_{0\infty}$, and n_* are the empirical constants. Equation (2.29) can be re-written as

$$\Delta T = T_w - T_\infty = c_0 r^{n_*} \quad (\text{for } \; c_0 = c_{0w} - c_{0\infty}), \tag{2.30}$$

$$\text{or} \quad \Delta T = c_{0w}(1-\beta) r^{n_*}. \tag{2.31}$$

Equations (2.1)–(2.4) and (2.12) (for $\partial T/\partial t = 0$), with allowance for Eq. (2.16), reduce to a self-similar form:

$$F^2 - G^2 + F'H = \frac{N^2 - \beta^2}{(1+N)^2} + F'', \tag{2.32}$$

$$2FG + G'H = G'', \tag{2.33}$$

$$HH' = P' + H'', \tag{2.34}$$

$$2F + H' = 0, \tag{2.35}$$

$$\theta'' - Pr(n_* F\theta + H\theta') = 0. \tag{2.36}$$

Here, $N = a/\omega = \text{const}$. A solution of Eqs. (2.32)–(2.35) for simultaneously non-zero values of β and N does not exist. However, such a solution can be found either for $N \neq 0$ and $\beta = 0$, or for $\beta \neq 0$ and $N = 0$.

Equations (2.32)–(2.36) have been often solved with the help of so-called in-house computer codes using a spectral collocation method based on the Chebyshev polynomials [13–18], Keller box [19] or quasi-linearization method [20], expansions in power/exponential series [9, 21], finite difference schemes [22], shooting methods [1, 8, 10, 12, 23], etc. Computer mathematics softwares like Mathcad, Mathlab, Mathematica, etc. enable solving Eqs. (2.32)–(2.36) via user interface programing options [3, 20].

A self-similar energy equation involving dissipation terms allows using only one value of the exponent $n_* = 2$ in the boundary conditions (2.29)–(2.31) [1, 2, 4]. At subsonic flow of air, dissipation effects, as well as radial heat conduction, are negligible. Therefore, we neglected the respective terms in Eq. (2.36) of the thermal boundary layer, which enabled us using arbitrary values of the parameter n_*.

Exact solutions of Eqs. (2.32)–(2.36) serve as benchmark datasets used in validations of experiments or CFD models developed for more complicated problems. Based on the self-similar solutions, it is also possible to develop approximate analytical solutions of problems, whose boundary conditions differ from Eqs. (2.27)–(2.31).

2.2.2 *Approximate Analytical Methods for Laminar Flow*

Laminar impingement flow over a single rotating disk at N = const. and $\beta = 0$ was simulated using an approximate mathematical method of Slezkin-Targ in [4]. Velocity components were approximated by sixth-order polynomials. A polynomial of third order resulted in an inaccuracy in the surface friction of up to $\sim$25 % at $N = 5$. This inaccuracy increases fast for higher values of N. Should the author [4] extend this method to model heat transfer? This would yield a cumbersome solution for the Nusselt number.

A complex combination of exponential and logarithmic functions resulted in an approximate solution for laminar flow over a single rotating disk [24]. The heat transfer problem was not solved. Such an extension of the method [24] would, however, yield even more inconvenient and cumbersome relations for the Nusselt number than in [4].

For porous injection through a rotating disk, an approximate solution was presented as a combined expansion in power and exponential series. It is obvious that this approach has the same deficiencies as the aforementioned methods [4, 24].

Analytical solutions [19] were obtained for a stretching disk for (a) a case of no rotation and (b) infinitely large stretching rate. Both situations have very limiting application; a general analytical solution for a stretching rotating disk does not exist.

Based on the above, one can conclude that a search for an exact analytical solution for the velocity, pressure, and temperature profiles in laminar flow over a rotating disk is a very complicated and inexpedient mathematical task. Alternatively, as demonstrated below, a match of an integral method and a

self-similar solution yields a transparent and accurate approximate analytical solution for fluid flow and heat transfer characteristics.

2.2.3 Numerical Methods

At early stages, finite difference methods implemented in in-house codes were used by different authors [25–38] to simulate laminar/turbulent fluid flow and heat transfer in rotating cavities formed by parallel co-rotating disks using algebraic [39] or low-Reynolds-number k-ε turbulence models [40–42]. A finite difference method was employed by the author [43] to simulate a 3D air flow in a rotating-disk grinder of solid particles with the RANS approach with a k-ε turbulence model [44].

Commercial CFD codes (e.g., FLUENT, CFX, Phoenics, etc.) using RANS approaches have been widely used by different authors to simulate fluid flow in rotating-disk systems [33, 36, 45–52]. Turbulence was modeled using closure with standard and realizable k-ε models, RNG k-ε model, k-ω SST model, Spalart–Allmaras model, and others.

The LES approach was employed by [53] to simulate a stationary turbulent flow over a rotating disk. The LES approach was also used in [54–58] to simulate turbulent flow and heat transfer over a single disk in air flow parallel to the disk surface.

Numerical simulation using in-house or commercial CFD codes is the most widely used universal tool for problems with arbitrary geometry and boundary conditions to be performed in academic and especially applied/industrial research. Given a proper mesh, accuracy of results depends here on the selection of the turbulence model, which is to be performed individually for each problem to be solved.

A disadvantage of CFD modeling is that it provides only an array of numerical data, which is often an inconvenience in comparison with analytical solutions. Therefore, methods delivering exact or approximate analytical solutions are advantageous for relatively simple geometries and boundary conditions.

2.3 Integral Methods

2.3.1 Momentum Boundary Layer

In frames of an integral method, Eqs. (2.17)–(2.23) are solved accompanied with models for (a) velocity/temperature profiles (or enthalpy thickness), as well as (b) shear stresses on the wall (velocity boundary layer) and wall heat flux (thermal boundary layer).

To briefly outline a history of the integral methods for rotating-disk systems, fundamentals of them were laid by von Karman [9] and Dorfman [4]. Further

development of model assumptions for integral methods was done in the works [1, 2, 48, 59]. An important feature of the method [1, 2] further elaborated in the present work consists in the use of the same mathematical form of the models for laminar or turbulent flow, which differ from each other only by numerical values of certain parameters. In fact, this confirms the idea of Loytsyanskiy [60], who said that there exists "an analogy between basic characteristics of laminar and turbulent boundary layers."

The radial v_r and tangential v_φ velocity components in the boundary layer are interrelated in accordance with the equation [61]

$$\bar{v}_r = \bar{v}_\varphi \tan \varphi. \tag{2.37}$$

In case where potential flow in the r-direction is negligible, i.e., $v_{r,\infty} = 0$, approximations of the velocity profiles were written by the authors [1, 2] in the following form:

$$\bar{v}_\varphi = 1 - g(\xi), \quad \bar{v}_r = \alpha f(\xi), \tag{2.38}$$

where the functions $g(\xi)$ and $f(\xi)$ of the variable $\xi = z/\delta$ were set to be independent of the coordinate r. For laminar flow,

$$g(\xi) = G_0(\xi), \quad f(\xi) = F_0(\xi)/\alpha_0. \tag{2.39}$$

The functions $G_0(\xi)$ and $F_0(\xi)$ are a solution of Eqs. (2.32)–(2.35) for a free rotating disk, i.e., for $N = 0$ and $\beta = 0$ [1, 2, 4].

For turbulent flow, power-law profiles were employed:

$$g(\xi) = 1 - \xi^n, \tag{2.40}$$

$$f(\xi) = \xi^n(1 - \xi), \quad \tan \varphi = \alpha(1 - \xi), \tag{2.41}$$

where n = 1/5–1/10 [1, 2, 4, 9, 48, 59, 62–64]. Approximations (2.40) and (2.41) were formulated for the first time by von Karman [9]. The characteristic Reynolds number determines the value of the exponent n (see Figs. 2.2, 2.3 and 2.4).

A more accurate approximation for $f(\xi)$ in turbulent flow is [65–68]

$$f(\xi) = \xi^n(1 - \xi)^2, \quad \tan \varphi = \alpha(1 - \xi)^2. \tag{2.42}$$

Nevertheless, Eq. (2.42) has been rarely used apparently due to the somewhat more complicated form of expressions resulting from the integration of Eqs. (2.17)–(2.19).

More elaborate power-law profiles were used by the authors [69]

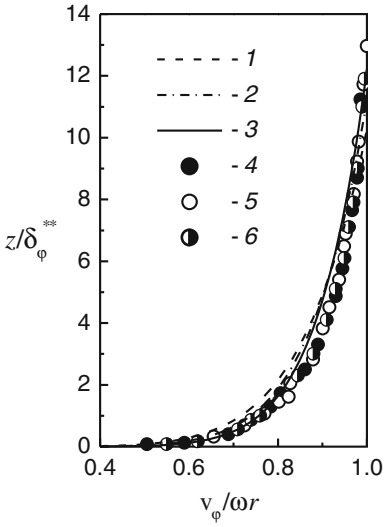

Fig. 2.2 Profiles of the non-dimensional tangential velocity in the turbulent boundary layer over a free rotating disk [3]. Calculation by Eq. (2.40) [61]: *1*—n = 1/7, *2*—1/8, *3*—1/9. Experiments: *4*—Re_ω = (0.4–1.6) × 10^6 [70], *5*—(0.6–1.0) × 10^6 [71], *6*—(0.65–1.0) × 10^6 [72]. Here $\delta_\varphi^{**} = \int_0^b \frac{v_\varphi}{\omega r}(1 - \frac{v_\varphi}{\omega r})\mathrm{d}z$ (definition of [70–74])

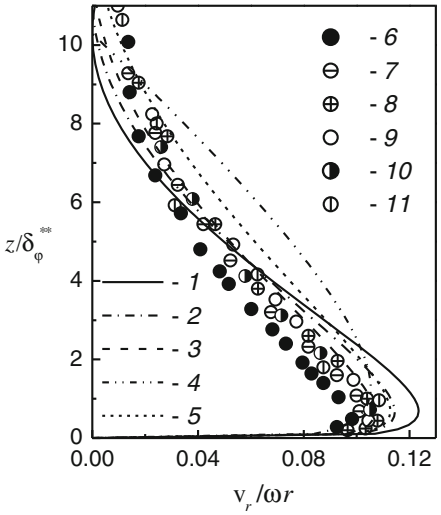

Fig. 2.3 Profiles of the non-dimensional radial velocity in the turbulent boundary layer over a free rotating disk [3]. Calculation by Eq. (2.42) or (2.58) [61]: *1*—n = 1/7, *2*—1/8, *3*—1/9. Equation (2.41), [9]: *4*—n = 1/7. Equation (2.44): *5*—n = 1/7, b = 0.7, c = 1.2, α = 0.2003. Experiments: *6*—Re_ω = 0.4 × 10^6, *7*—0.65 × 10^6, *8*—0.94 × 10^6, *9*—1.6 × 10^6 [70], *10*—0.6 × 10^6, *11*—1.0 × 10^6 [71]

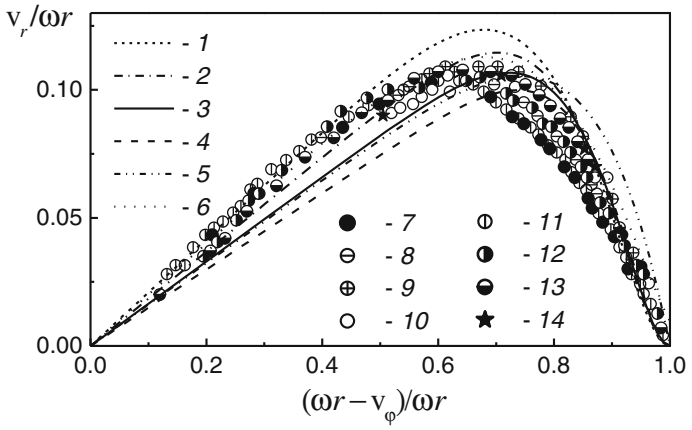

Fig. 2.4 Correlation between the radial and tangential velocity components in the boundary layer [3]. Calculation by Eq. (2.59) at $L = 2$ (curves *1–4*) or $L = 1$ (curve *5*) [61]: *1*—$n = 1/7$, *2*—1/8, *3*—1/9, *4*—1/10, *5*—1/7, von Karman's method [9], *6*—1/7, Eq. (2.44) for $b = 0.7$, $c = 1.2$, $\alpha = 0.2003$. Experiments: *7*—$Re_\omega = 0.4 \times 10^6$, *8*—$0.65 \times 10^6$, *9*—$0.94 \times 10^6$, *10*—$1.6 \times 10^6$ [70], *11*—0.4×10^6, *12*—0.6×10^6, *13*—1.0×10^6 [71], *14*—2.0×10^6 [75]

$$f(\xi) = \xi^n(1 - \xi^{n/m}), \quad \tan\varphi = \alpha(1 - \xi^{n/m}), \tag{2.43}$$

with exponents n and m independent from each other. The authors [69] have not further developed their model, apparently because of its excessively complicated structure.

A trigonometric function approximating the function $\tan\varphi$ in Eq. (2.37)

$$\tan\varphi = \alpha[(1 - \sin^b(c\xi)] \tag{2.44}$$

was used by [76, 77]. The values of the constants $b = 0.7$, $c = 0.12$ at $n = 1/7$, and $b = 0.697$, $c = 0.117$ at $n = 1/8$ mentioned in [76] are, however, erroneous.

For instance, for $b = 0.7$ at $n = 1/7$, one must use a value of $c = 1.2$ (Figs. 2.3 and 2.4). The model [76, 77] is more complicated than the von Karman's approach. Expressions for the Nusselt number that could have been obtained (but actually have not been obtained!) on the base of the model (2.44) would have been again too cumbersome.

For N = const., the following relations were used in [78] and [79–81], respectively:

$$\tan\varphi = \alpha + (N - \alpha)\xi, \tag{2.45}$$

$$\tan\varphi = \alpha(1 - \xi) + \kappa, \tag{2.46}$$

where $\kappa = \dot{m}/[2\pi\rho sr(1-\beta)\omega r]$. Equation (2.46) is least justified, since it does not agree with the condition $\tan\varphi_w = \alpha$ and complicates the solution of Eqs. (2.17) and (2.18).

Thus, Eqs. (2.43)–(2.46) demonstrate lower accuracy than models (2.37)–(2.45).

Integration of Eqs. (2.17) and (2.18) in view of Eqs. (2.37)–(2.45) yields ordinary differential equations with the unknown variables $\alpha(r)$ and $\delta(r)$ for a pre-set function of $\beta(r)$, or $\alpha(r)$ and $\beta(r)$ for a pre-set function $\delta(r)$. In view of an assumption N = const. or β = const., the parameter α becomes constant as well. In this case, δ = const. in laminar flow, or $\delta \sim r^m$ in turbulent flow [1, 2, 4].

Given the velocity profiles in the form of power-law functions, shear stresses τ_{wr} and $\tau_{w\varphi}$ on the right-hand sides of Eqs. (2.17)–(2.19) can be written as [1, 2, 4]

$$\tau_{wr} = -\alpha\tau_{w\varphi}, \quad \tau_{w\varphi} = -\mathrm{sgn}(1-\beta)\tau_w(1+\alpha^2)^{1/2}, \tag{2.47}$$

$$c_f = C_n^{-2/(n+1)} Re_{V_*}^{-2n/(n+1)}, \tag{2.48}$$

$$C_n = 2.28 + 0.924/n. \tag{2.49}$$

Equation (2.49) was proposed in [69]. The constant C_n takes the values 8.74, 9.71, 10.6, and 11.5 for n = 1/7, 1/8, 1/9, and 1/10, accordingly [1, 2, 4, 9, 69].

In frames of logarithmic models of the velocity profiles [82], their near-wall approximations look as

$$v_r = \alpha\omega r + \frac{2.5\alpha V_\tau}{(1+\alpha^2)^{1/2}}\ln(\xi), \quad v_\varphi = -\frac{2.5V_\tau}{(1+\alpha^2)^{1/2}}\ln(\xi). \tag{2.50}$$

A validation of the logarithmic model has been performed only for a free disk, with the heat transfer problem being not modeled. The moment coefficient C_M is given by a transcendental algebraic equation (see Sect. 3.3) [82]. Inconvenience and complexity prevented further development and use of the logarithmic approach [82].

The integral method described in the work [48] and references includes special arrangements for rotor–stator systems, which fall out of the scope of the present work.

2.3.2 *Thermal Boundary Layer*

Heat transfer modeling in the frames of integral methods performed in the majority of the known works [1, 2, 4, 9, 48, 64, 68, 79–81, 83–89] was based on a "theory of local modelling" (which is a direct translation of the name used in the Russian language literature) that stems from the method of Loytsyanskiy [60] (see also [90]). This theory was for the first time applied to rotating-disk systems by Dorfman [4], who postulated a so-called heat transfer law for the Stanton number:

$$St = M_s Re_T^{**-\sigma} Pr^{-n_s}. \tag{2.51}$$

Universal constants M_s, σ, and n_s do not depend on the disk surface temperature T_w and the Prandtl number. These constants take the values $\sigma = 0.25$, $n_s = 0.5$, and $M_s = 7.246 \times 10^{-3}$ for turbulent flow, and $\sigma = 1.0$, $n_s = 1.0$, and $M_s = 0.07303$ for laminar flow [1–4]. Equation (2.51) is substituted into the thermal boundary layer Eq. (2.23). In doing so, the only remaining unknown parameter is δ_T^{**}.

In the books [1, 2], the Reynolds analogy parameter χ was involved in the integral method instead of the enthalpy thickness δ_T^{**}

$$\frac{q_w}{\tau_{w\phi}} = \chi \frac{c_p(T_\infty - T_w)}{\omega r(1-\beta)}. \tag{2.52}$$

The unknown parameter χ was found as a result of the solution of Eq. (2.23) by the authors [1, 2] based on the models (2.51) and (2.52).

A power-law temperature profile in turbulent flow regime at $n_T = 1/5$

$$\Theta = \frac{T - T_w}{T_\infty - T_w} = \xi_T^{n_T}, \quad \theta = \frac{T - T_\infty}{T_w - T_\infty} = 1 - \Theta = 1 - \xi_T^{n_T} \tag{2.53}$$

was employed in the work [63], which for a long time had been the only one that used the model (2.53). An additional assumption $\Delta = \delta_T/\delta = 6$ at $T_w = \text{const}$. used in the work [63] is apparently erroneous and must be replaced with a model that enables finding the parameter Δ and its dependence on the other factors (like the model described in Sect. 2.4).

2.4 Improved Integral Method

2.4.1 Structure of the Method

Original results of the studies of fluid flow and heat transfer in rotating-disk configurations outlined here stem from the investigations performed using an improved integral method developed by the author of this work and described in the publications [3, 5, 61, 91–109]. Throughout this work, this methodology is always named as ***the present integral method***.

The basic statements of the present integral method are

(a) the system of Eqs. (2.17)–(2.23);
(b) turbulent velocity and temperature profiles given by improved approximations;
(c) a novel enthalpy thickness model for laminar/turbulent flow;
(d) power-law model for shear stresses and heat fluxes on the wall; and
(e) specified disk temperature distribution, together with the boundary conditions for the temperature and velocity in inviscid (i.e., potential) flow.

The present integral method employs the bedrock assumption that the same mathematical model can be used for modeling laminar and turbulent boundary layers, where the difference is made by numerical values of the certain empirical constants of the model. This model is a mathematical expression of the analogy between the basic characteristics of the laminar and turbulent flow under the same boundary conditions [60]. Authors [1, 2, 4, 9] have already validated this idea with respect to convective heat transfer in rotating-disk systems. However, the imperfect mathematical model used in these works caused noticeable inaccuracy in the simulation of heat transfer under certain thermal boundary conditions (see Sect. 3.2 of Chap. 3).

In the present integral method, we do not attempt to use power-law approximations of the velocity/temperature profiles in laminar flow, which involve polynomials of seventh order or higher and result in cumbersome equations for the friction coefficient and the Nusselt number. We wish to make use of simple and transparent power-law relations for the friction coefficient and the Nusselt number derived using power-law models of the velocity/temperature profiles for turbulent flow. Mathematical expressions for these parameters for turbulent flow can be extended onto laminar flow with particular constants remaining unknowns to be found empirically via validations against the exact solution.

Consequently, the logic of the method is following: firstly, an integral method for turbulent boundary layer is created and validated against experiments; and secondly, the mathematical form of the integral method is elaborated and validated for laminar flow.

2.4.2 *Turbulent Flow: Velocity and Temperature Profiles*

Velocity profiles are approximated using power-law models, Eq. (2.37) for v_r, as well as the first of Eqs. (2.38) and (2.40) for v_φ. A quadratic polynomial approximates the tangent of the flow swirl angle $\tan\varphi$. The coefficients a, b, and c must comply with the boundary conditions at the wall and at the outer edge of the boundary layer

$$\tan\varphi = a + b\xi + c\xi^2, \tag{2.54}$$

$$\xi = 0, \quad \tan\varphi = \tan\varphi_w = \alpha, \tag{2.55}$$

$$\xi = 1, \quad \tan\varphi = \tan\varphi_\infty = v_{r,\infty}/(\omega r - v_{\varphi,\infty}) = N/(1-\beta) = \kappa, \tag{2.56}$$

$$\xi = 1, \quad \mathrm{d}(\tan\varphi)/\mathrm{d}\xi = 0. \tag{2.57}$$

Conditions (2.54)–(2.57) yield

$$a = \alpha, \quad b = -2(\alpha - \kappa), \quad c = \alpha - \kappa, \quad (\tan\varphi - \kappa)/(\alpha - \kappa) = (1 - \xi)^2. \tag{2.58}$$

Figures 2.2 and 2.3 show profiles of the radial and tangential velocity components for a free rotating disk ($\kappa = 0$) calculated by Eqs. (2.37) and (2.58).

The present integral method enabled finding wall values of the tangent of the flow swirl angle α presented in Table 3.4 of Chap. 3 in comparison with α values obtained by von Karman's method [9]. Power-law profiles for the $\bar{v}_r$ and $\bar{v}_\varphi$ jointly with a quadratic Eq. (2.58) for tan φ agree well with experiments in the outer part of the boundary layer. Here, the profiles at $n = 1/9$ agree with the experiments [70, 71] (Figs. 2.2 and 2.3). The same trend demonstrates Fig. 2.4, where velocity components $\bar{v}_r$ on $\bar{v}_\varphi$ are interconnected via an equation resulting from Eqs. (2.37), (2.38), (2.40), and (2.58) [61]:

$$\bar{v}_r = \alpha\,\bar{v}_\varphi(1 - \bar{v}_\varphi^{1/n})^L. \tag{2.59}$$

Here, $L = 2$ in the present method and $L = 1$ in the method [9]. In the vicinity of the wall, the value of the exponent $n = 1/7$–$1/8$ yields, however, the best agreement with experiments. Based on Eq. (2.59) [61], a maximum in the dependence of $\bar{v}_r$ on $\bar{v}_\varphi$ is observed at

$$\bar{v}_{\varphi,\max} = \xi_{\max}^n, \quad \xi_{\max} = n/(n + L). \tag{2.60}$$

In frames of the present integral method, temperature distributions in the boundary layer are approximated with Eq. (2.53). This appears to be in a good agreement with the experimental data of different authors depicted in Fig. 2.5.

2.4.3 Surface Friction and Heat Transfer

Shear stresses $\tau_{w\varphi}$, τ_{wr} and wall heat flux q_w can be expressed with the help of a two-layer model of the velocity and temperature profiles non-dimensionalized using the law of the wall. Power-law profiles (2.40) and (2.53) can be re-written in wall coordinates as

$$V^+ = \xi^n/\sqrt{c_f/2}, \quad T^+ = \xi_T^{n_T}\sqrt{c_f/2}/St. \tag{2.61}$$

These relations are not valid in the viscous sub-layer; therefore, their place is taken here by the linear equations

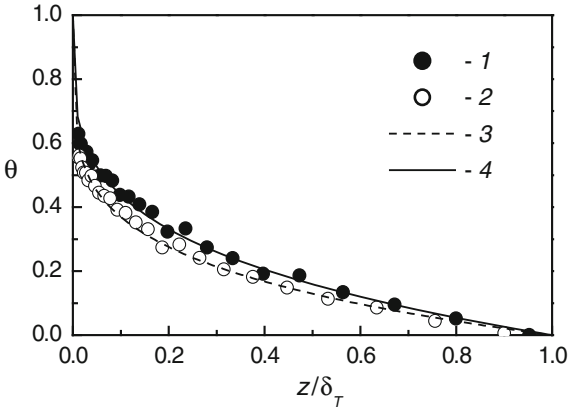

Fig. 2.5 Profiles of the non-dimensional temperature θ in the turbulent boundary layer over a free rotating disk [3]. Experiments [72], q_w = const., $Re_\omega = 1.0 \times 10^6$: *1*—inner heater on, *2*—inner heater off. Calculations by Eq. (2.53): *3*—n_T = 1/5, *4*—1/4

$$V^+ = z^+, \quad T^+ = Pr\, z^+. \tag{2.62}$$

Equations (2.61) and (2.62) must be spliced at the boundary z_1^+ of the viscous sub-layer and at the boundary z_{1T}^+ of the heat conduction sub-layer, accordingly. In doing so, one can come to relations for the friction coefficient and the Stanton number:

$$c_f/2 = (z_1^+)^{2(n-1)/(n+1)}\, Re_{V_*}^{-2n/(n+1)}, \tag{2.63}$$

$$St = (z_1^+)^{n_T-1} Re_{V*}^{-n_T} (c_f/2)^{(1-n_T)/2} \Delta^{-n_T} (z_{1T}^+/z_1^+)^{n_T-1} Pr^{-n_T}. \tag{2.64}$$

Instead of the coordinate z_1^+, its modification $C_n = (z_1^+)^{1-n}$ is often used. C_n is a constant whose dependence on the exponent n is clarified in the comments to Eq. (2.49). The constant z_1^+ takes the values 12.54, 13.44, 14.23, and 15.09 for n = 1/7, 1/8, 1/9, and 1/10, respectively. Based on Eq. (2.47), shear stresses τ_w, $\tau_{w\varphi}$, and τ_{wr} are mutually related as

$$\tau_{wr}/\rho = C_n^{-2/(n+1)} \mathrm{sgn}(1-\beta)(v/\delta)^{2n/(n-1)} (\omega r|1-\beta|)^{2/(n-1)} \alpha (1+\alpha^2)^{0.5(1-n)/(1+n)},$$

$$\tau_{w\phi}/\rho = -C_n^{-2/(n+1)} \mathrm{sgn}(1-\beta)(v/\delta)^{2n/(n-1)} (\omega r|1-\beta|)^{2/(n-1)} \times (1+\alpha^2)^{0.5(1-n)/(1+n)}. \tag{2.65}$$

In Eq. (2.64), the unknown Δ to be found is a function of the Prandtl number Pr, as well as the distribution of $T_w(r)$. The ratio (z_{1T}^+/z_1^+) depends on the Pr number

only. One can denote $(z_{1T}^{+}/z_{1}^{+})^{n_T-1}Pr^{-n_T} = Pr^{-n_p}$, with the exponent n_p remaining so far unknown.

A condition $n_T = n$ will be often employed below, which leads to a simplification of the expressions for the Stanton number and the Nusselt number:

$$St = (c_f/2)\Delta^{-n}Pr^{-n_p}, \tag{2.66}$$

$$Nu = St\frac{V_* r}{\nu}Pr = St\, Re_\omega Pr|\beta - 1|(1+\alpha^2)^{1/2}. \tag{2.67}$$

2.4.3.1 Integral Equations

Having integrated Eqs. (2.17) and (2.18) with respect to the z-coordinate in view of Eqs. (2.37)–(2.40), (2.58), one can derive the following ordinary differential equations [61]:

$$\begin{aligned}&\frac{\mathrm{d}}{\mathrm{d}r}\left\{\delta r(\omega r)^2(1-\beta)^2\left[\kappa(A_1\alpha + A_2\kappa) - \left(B_1\alpha^2 + B_2\alpha\kappa + B_3\kappa^2\right)\right]\right\}\\ &\quad + \delta\omega r^2(1-\beta)\frac{\mathrm{d}(N\omega r)}{\mathrm{d}r}\left[\kappa - (A_1\alpha + A_2\kappa)\right]\\ &\quad + \rho\delta(\omega r)^2\left(C_1 + C_2\beta + C_3\beta^2\right) = r\tau_{wr}/\rho,\end{aligned} \tag{2.68}$$

$$\begin{aligned}&\frac{\mathrm{d}}{\mathrm{d}r}\left\{\delta\omega^2 r^4(1-\beta)[\alpha(D_1 + \beta D_2) + \kappa(D_3 + \beta D_4)]\right\}\\ &\quad - (\omega r)^2\beta\frac{\mathrm{d}}{\mathrm{d}r}\left[\delta\omega r^2(1-\beta)(A_1\alpha + A_2\kappa)\right] = -r^2\tau_{w\varphi}/\rho,\end{aligned} \tag{2.69}$$

where

$$\begin{aligned}&A_1 = 1/(n+1) - A_2; \quad A_2 = 2/(n+2) - 1/(n+3);\\ &B_1 = 1/(2n+1) - 2/(n+1) + 6/(2n+3) - 2/(n+2) + 1/(2n+5);\\ &B_2 = 2/(n+1) - 10/(2n+3) + 4/(n+2) - 2/(2n+5);\\ &B_3 = 4/(2n+3) - 2/(n+2) + 1/(2n+5);\\ &C_1 = 1 - 2/(n+1) + 1/(2n+1),\\ &C_2 = -2(1/(2n+1) - 1/(n+1));\\ &C_3 = -1 + 1/(2n+1);\\ &D_1 = A_1 - D_2;\\ &D_2 = 1/(2n+1) - D_4;\\ &D_3 = A_2 - D_4;\\ &D_4 = 1/(n+1) - 1/(2n+3).\end{aligned}$$

Equation (2.20) for the thermal boundary layer integrated with respect to z and account for Eqs. (2.37), (2.38), (2.40), (2.53), and (2.58) can be written as

$$\frac{\mathrm{d}}{\mathrm{d}r}\left[\delta\omega r^2(1-\beta)F_1(T_\infty - T_w)\right] + \frac{\mathrm{d}T_\infty}{\mathrm{d}r}\delta\omega r^2(1-\beta)F_2 = -St\ {}_*r\Delta^{-n_T}Pr^{-n_P}(T_\infty - T_w), \tag{2.70}$$

where

$$\begin{aligned}
F_1 &= E_1, \quad F_2 = E_2 \text{ at } \Delta \le 1;\ F_1 = E_3,\ F_2 = E_4 \text{ at } \Delta \ge 1;\\
E_1 &= \Delta^{n+1}(aa_{*T} + bb_{*T}\Delta + cc_{*T}\Delta^2),\\
a_{*T} &= 1/(1+n+n_T) - 1/(1+n),\\
b_{*T} &= 1/(2+n+n_T) - 1/(2+n),\\
c_{*T} &= 1/(3+n+n_T) - 1/(3+n),\\
E_2 &= \Delta^{n+1}[a/(n+1) + b\Delta/(n+2) + c\Delta^2/(n+3)],\\
E_3 &= E_5 + \kappa E_6,\\
E_4 &= \alpha A_1 + \kappa(\Delta - 1) + \kappa A_2,\\
E_5 &= \alpha(-A_1 + \Delta^{-n_T}D_{2T}),\\
D_{2T} &= 1/(1+n+n_T) - D_{4T},\\
E_6 &= (\Delta - \Delta^{-n_T})/(n_T+1) - \Delta + 1 - A_2 + \Delta^{-n_T}D_{4T},\\
D_{4T} &= 2/(2+n+n_T) - 1/(3+n+n_T).
\end{aligned}$$

The mass flow rate through the boundary layer can be expressed as

$$\dot{m}_d/(\rho\omega r^3) = 2\pi(1-\beta)(A_1\alpha + A_2\kappa)\delta/r. \tag{2.71}$$

Equations (2.68)–(2.70) involve three unknowns:

(a) *in the entraining boundary layers*: α, δ, and Δ for specified β, as well as T_∞; and
(b) *in the Ekman-type boundary layers*: α, β for a specified mass flowrate $\dot{m}_d$ = const. (i.e., specified distribution of δ), as well as unknown T_∞ for a specified Δ = const.

In case (a), Eqs. (2.68)–(2.70) can be solved analytically at the boundary conditions (2.27)–(2.31) (and N = const.), assumptions α = const. and Δ = const. and a power law for the radial distribution of the boundary layer thickness $\delta \sim r^m$. If the boundary conditions are approximated with arbitrary functions, Eqs. (2.68)–(2.70) are to be solved numerically being re-written to a notation that enables using the Runge–Kutta method [92, 96]:

$$\begin{cases} \alpha' = (\Phi_1\Phi_4 + \Phi_2)/(1 - \Phi_1\Phi_3), \\ \bar{\delta}' = (\Phi_2\Phi_3 + \Phi_4)/(1 - \Phi_1\Phi_3), \end{cases} \tag{2.72}$$

$$\Delta' = (S_1 - S_2 - S_3)/S_4. \tag{2.73}$$

Here,

$$\begin{aligned}
\Phi_2 &= \{[\mathrm{sgn}(1-\beta)|c_{\mathrm{fr}}/2|\bar{r}^3 Re_{V_*}^2/\bar{\delta}^2 - Z_1\bar{\delta} \\
&\quad - G_1\bar{\delta} - G_2]/(\bar{\delta}\bar{r}) - Q_2\bar{r}^2\}/Q_1; \\
\Phi_4 &= \{-\mathrm{sgn}(1-\beta)|c_{f\varphi}/2|\bar{r}^2 Re_{V_*}^2/\bar{\delta}^2 - \bar{\delta}[\alpha Q_3' + \bar{Q}_4' \\
&\quad + (\beta Re_\omega)'(\alpha Q_5 + Q_6)]/Q_7\}; \\
\Phi_1 &= -Z_1/(\bar{\delta}Q_1);\ \Phi_3 = -\bar{\delta}Q_3/Q_7; \\
Z_1 &= Re_\omega^2(1-\beta)^2[-B_1\alpha^2 + \alpha\kappa(A_1 - B_2) + \kappa^2(A_2 - B_3)]; \\
G_1 &= Re_\omega^2(C_1 + C_2\beta + C_3\beta^2); \\
G_2 &= Re_\omega^2(1-\beta)\bar{\delta}[-A_1\alpha + \kappa(1 - A_2)]\bar{v}_{r,\infty}'; \\
Q_1 &= Re_\omega^2(1-\beta)^2[-2\alpha B_1 + \kappa(A_1 - B_2)];\ Q_3 = -Re_\omega^2(1-\beta)^2 D_1 \\
Q_2 &= Re_{\omega i}^2\{-\alpha^2 B_1[\bar{r}^2(1-\beta)^2]' \\
&\quad + \alpha(A_1 - B_2)[\bar{r}(1-\beta)\bar{v}_{r,\infty}]' + (A_2 - B_3)(\bar{v}_{r,\infty}^2)'\}; \\
Q_4 &= -Re_\omega^2(1-\beta)\bar{v}_{r,\infty}D_3/\bar{r};\ Q_5 = -Re_\omega(1-\beta)A_1; \\
Q_6 &= -Re_{\omega i}\bar{r}\bar{v}_{r,\infty}A_2;\ Q_7 = \alpha Q_3 + Q_4; \\
\bar{v}_{r,\infty} &= v_{r,\infty}/v_{r,\infty}(\omega a);\ Re_{\omega i} = \omega r_i^2/\nu;\ |c_{fr}/2| = (c_f/2)\alpha/(1+\alpha^2)^{1/2}; \\
|c_{f\varphi}/2| &= (c_f/2)/(1+\alpha^2)^{1/2};\ \bar{\delta} = \delta/r_i;\ \bar{r} = r/r_i.
\end{aligned}$$

Given $\Delta \le 1$ in Eq. (2.73), we have

$$\begin{aligned}
S_1 &= -Re_\omega|1-\beta|(1+\alpha^2)^{1/2}St(\bar{T}_\infty - \bar{T}_w); \\
S_2 &= \bar{T}_\infty'\bar{\delta}Re_\omega\Delta^{n+1}[\alpha(1-\beta)/(n+1) - 2\Delta(\alpha(1-\beta) - N)/(n+2) \\
&\quad + \Delta^2(\alpha(1-\beta) - N)/(n+3)]; \\
S_3 &= \Delta^{n+1}L_1' + \Delta^{n+2}L_2' + \Delta^{n+3}L_3';\ S_4 = L_1(n+1)\Delta^n + L_2(n+2)\Delta^{n+1} + L_3(n+3)\Delta^{n+2}; \\
L_1 &= L_0 a_{*T}\alpha(1-\beta);\ L_2 = L_0 b_{*T}(-2)[\alpha(1-\beta) - N];\ L_3 = L_0 c_{*T}[\alpha(1-\beta) - N]; \\
L_0 &= \bar{\delta}Re_\omega(\bar{T}_\infty - \bar{T}_w),\ \bar{T} = T/T_{\mathrm{ref}}.
\end{aligned}$$

The function S_1 has the identical form for $\Delta \geq 1$ and $\Delta \leq 1$.

$$\begin{aligned}
\text{For } \Delta \geq 1: \; S_2 &= \bar{T}'_\infty \bar{\delta} Re_\omega [\alpha(1-\beta)A_1 + NA_2 + N(\Delta - 1)]; \\
S_3 &= L'_{1*} C^*_{6T} + L'_{2*} C^*_{7T}; \\
S_4 &= -n_T \Delta^{-n_T - 1} D_{2T} L_{1*} + [(1 + n_T \Delta^{-n_T - 1})/(n_T + 1) \\
&\quad - D_{4T} n_T \Delta^{-n_T - 1} - 1] L_{2*}; \\
L_{1*} &= L_0(1-\beta)\alpha; \\
L_{2*} &= L_0 N; \\
C^*_{6T} &= -A_1 + \Delta^{-n_T} D_{2T}; \\
C^*_{7T} &= (\Delta - \Delta^{-n_T})/(n_T + 1) - \Delta + 1 - A_2 + D_{4T} \Delta^{-n_T}.
\end{aligned}$$

Derivatives with respect to the radial coordinate $\mathrm{d}/\mathrm{d}\bar{r}$ are denoted here with primes; r_i is a characteristic radius (for instance, the inlet radius that is used here).

In case (b), i.e., in the Ekman-type layers

$$\begin{cases}
\alpha' = \frac{c_f}{2}\alpha(\beta - 1) Re_\omega (1 + \alpha^2)^{1/2} \frac{4\pi A_1 r_i}{B_1 C_w b} + \frac{\mathrm{d}\beta}{\mathrm{d}\bar{r}} \frac{\alpha}{\beta - 1} - \frac{C_3[\beta + n/(n+1)]}{\bar{r}(\beta - 1)\alpha B_1} - \frac{\alpha}{\bar{r}}, \\
\beta' = \left\{ -\frac{c_f}{2}(1-\beta)^2 Re_\omega (1 + \alpha^2)^{1/2} \frac{4\pi A_1 r_i}{D_1 C_w b} - \frac{2}{\bar{r}} \left[\beta \left(1 - \frac{A_1}{D_1} \right) - 1 \right] \right\} \Big/ \left(1 - \frac{A_1}{D_1} \right),
\end{cases} \tag{2.74}$$

$$\frac{\mathrm{d}\bar{T}_\infty}{\mathrm{d}\bar{r}} = \left[St \frac{V_* r}{\nu} \frac{2\pi}{0.5 C_w} \frac{r_i}{b} \frac{1}{K_H} (\bar{T}_\infty - \bar{T}_w) + \frac{\mathrm{d}\bar{T}_w}{\mathrm{d}\bar{r}} \right] \frac{K_H}{K_H - 1}. \tag{2.75}$$

In the Ekman-type layers, authors [1, 2] recommended to assign the parameter K_H to be constant [92, 95, 97]:

$$K_H = 1 - (D_{2T}/A_1)\Delta^{-n_T} = \text{const.} \quad \text{or} \quad \Delta = \text{const.} \tag{2.76}$$

2.5 Disk Rotation in a Fluid Rotating as a Solid Body and Simultaneous Accelerating Imposed Radial Flow

We will consider here flows where β = const., N = const., and $\kappa > 0$. The assumption β = const. outlines the solid-body rotation case that occurs in rotor–stator geometries. The assumption N = const. describes the case of accelerating radial flow, which occurs around the stagnation point of flow impinging onto a perpendicular plate. If $\kappa > 0$, fluid flow over a rotating disk never exhibits recirculation [1, 2, 68]. Given these assumptions, one can solve Eqs. (2.68) and (2.69) analytically. This solution can be written as [3]

$$\delta = C_\delta r^m, \quad C_\delta = \gamma(\omega/\nu)^{-2n/(3n+1)}, \quad \delta/r = \gamma Re_\omega^{-2n/(3n+1)}, \tag{2.77}$$

$$\alpha = \text{const.}, \quad m = (1-n)/(3n+1), \tag{2.78}$$

$$\gamma = \gamma_* |1-\beta|^{(1-n)/(3n+1)}, \tag{2.79}$$

$$C_\text{M} = \varepsilon_M Re_\varphi^{-2n/(3n+1)}, \tag{2.80}$$

$$\dot{m}_\text{d}/(\mu r) = \varepsilon_m Re_\omega^{(n+1)/(3n+1)}, \tag{2.81}$$

$$c_f/2 = A_c Re_\omega^{-2n/(3n+1)}, \tag{2.82}$$

$$\alpha = -H_2/2H_3 + [(H_2/2H_3)^2 - H_1/H_3]^{1/2}, \tag{2.83}$$

$$\gamma_* = C_n^{-2/(3n+1)}(1+\alpha^2)^{0.5(1-n)/(3n+1)} H_9^{-(n+1)/(3n+1)}, \tag{2.84}$$

$$\varepsilon_m = \varepsilon_m^* |1-\beta|^{2(n+1)/(3n+1)}, \quad \varepsilon_m^* = 2\pi\gamma(A_1\alpha + A_2\kappa)\text{sgn}(1-\beta), \tag{2.85}$$

$$\varepsilon_\text{M} = \frac{8\pi}{5-4n/(3n+1)} C_n^{-\frac{2}{n+1}} \gamma_*^{\frac{2n}{n+1}} |1-\beta|^{\frac{2(n-1)}{3n+1}} (1+\alpha^2)^{\frac{1-n}{2(n+1)}} \text{sgn}(1-\beta), \tag{2.86}$$

$$A_c = C_n^{-2/(n+1)} \gamma^{-2n/(n+1)} (1+\alpha^2)^{-n/(n+1)} |\beta-1|^{-2n/(n+1)}, \tag{2.87}$$

where

$$\begin{aligned}
&H_1 = C_3(\beta - C_5) + (\beta-1)\kappa^2 H_4;\ H_2 = \kappa(\beta H_5 + H_6);\\
&\quad H_3 = \beta H_7 + H_8;\\
&H_4 = 1 + (2+m)A_2 - (3+m)B_3;\ H_5 = A_1(2+m)\\
&\quad - B_2(3+m) + D_4(m+4) - A_2(2+m);\\
&H_6 = -A_1(2+m) + B_2(3+m) + D_3(4+m);\\
&H_7 = -(3+m)B_1 + (4+m)D_2 - (2+m)A_1;\\
&H_8 = (3+m)B_1 + (4+m)D_1; C_5 = C_1/C_3;\\
&H_9 = \alpha[(D_1 + \beta D_2)(4+m) - \beta(2+m)A_1]\\
&\quad + \kappa[(D_3 + \beta D_4)(4+m) - \beta A_2(2+m)].
\end{aligned} \tag{2.88}$$

Equation (2.70) can be solved analytically at the boundary conditions (2.29)–(2.31) provided that Δ = const., Pr = const., and $n = n_T$. An additional condition is $D_{2T} = D_2$ and $D_{4T} = D_4$.

Equation (2.70) is to be solved jointly with Eq. (2.69), in view of Eqs. (2.31), (2.67), (2.77) and (2.78). As a result, one can derive [91]

$$\left[F_1(2+m+n_*)+\frac{\beta n_*}{\beta-1}F_2\right]\Delta^n Pr^{n_p}=(4+m)C_4+\frac{2\beta}{\beta-1}C_5. \tag{2.89}$$

Functions F_1 and F_2 are clarified in explanations to Eq. (2.70); $C_4=-(\alpha D_1+\kappa D_2)$, $C_5=1/(n+1)+1/(n+2)+1/(n+3)$. Solutions of Eq. (2.89) for the cases $\Delta \geq 1$ and $\Delta \leq 1$ are different (which is manifested via different mathematical expressions for F_1 and F_2 at $\Delta \geq 1$ and $\Delta \leq 1$). Heat transfer conditions at $\Delta \geq 1$ can be observed for gases at $\mathrm{Pr} \leq 1$. Conditions with $\Delta \leq 1$ take place at heat transfer in liquids for $\mathrm{Pr} \geq 1$ (see Chap. 6).

Given simultaneously non-zero values of β and N, the algebraic Eq. (2.89) is transcendental. At $N = 0$ and $\Delta \geq 1$, there exists an explicit solution for the parameter Δ. The exponent n_p for flow over the free rotating disk is specified below.

Nusselt and Stanton numbers are given by the following equations:

$$St=A_c Re_\omega^{-2n/(3n+1)}\Delta^{-n}Pr^{-n_p}, \tag{2.90}$$

$$Nu=A_c(1+\alpha^2)^{1/2}|1-\beta|Re_\omega^{(n+1)/(3n+1)}\Delta^{-n}Pr^{1-n_p}. \tag{2.91}$$

The *present integral method* is thoroughly validated for turbulent air flow and extended to laminar flow in Chaps. 3 and 4. Simulations for a free rotating disk ($\beta = 0$, $N = 0$) are described in detail in Chap. 3. Cases of a rotating disk in a fluid that (a) co-rotates as a solid body (β = const., $N = 0$), and (b) is uniformly accelerating and non-rotating ($\beta = 0$, N = const.), as well as for the case of turbulent through flow between parallel co-rotating disks are analyzed in Chap. 4. A description of an extension of the integral method for gases and liquids at Prandtl or Schmidt numbers larger than unity is documented in Chap. 6.

References

1. Owen JM, Rogers RH (1989) Flow and heat transfer in rotating-disc systems. In: Rotor-stator systems, vol 1. Research Studies Press Ltd., Taunton
2. Owen JM, Rogers RH (1995) Flow and heat transfer in rotating-disc systems. In: Rotating cavities, vol 2. Research Studies Press Ltd., Taunton
3. Shevchuk IV (2009) Convective heat and mass transfer in rotating disk systems. Springer, Berlin
4. Dorfman LA (1963) Hydrodynamic resistance and the heat loss of rotating solids. Oliver and Boyd, Edinburgh
5. Shevchuk IV (2002) Laminar heat transfer in a rotating disk under conditions of forced air impingement cooling: approximate analytical solution. High Temp 40(5):684–692
6. Cochran WG (1934) The flow due to a rotating disk. Proc Cambridge Phil Soc 30:365–375
7. Ginzburg IP (1970) Theory of resistance and heat transfer. Izd. Leningrad. University, Leningrad, USSR (in Russian)
8. Hartnett JP, Deland EC (1961) The influence of Prandtl number on the heat transfer from rotating nonisothermal disks and cones. Trans ASME J Heat Transfer 83(1):95–96

9. Karman Th von (1921) Über laminare und turbulente Reibung. Z Angew Math Mech 1(4):233–252
10. Lin H-T, Lin L-K (1987) Heat transfer from a rotating cone or disk to fluids at any Prandtl number. Int Commun Heat Mass Transfer 14(3):323–332
11. Schlichting G (1968) Boundary-layer theory. McGraw-Hill Book Company, New York
12. Sparrow EM, Gregg JL (1959) Heat transfer from a rotating disc to fluids at any Prandtl number. Trans ASME J Heat Transfer 81:249–251
13. Turkyilmazoglu M (2010) Heat and mass transfer on the unsteady magnetohydrodynamic flow due to a porous rotating disk subject to a uniform outer radial flow. Trans ASME J Heat Transfer 132(6). Paper 061703
14. Turkyilmazoglu M (2011) Wall stretching in magnetohydrodynamics rotating flows in inertial and rotating frames. AIAA J Thermophys Heat Transfer 25(4):606–613
15. Turkyilmazoglu M (2011) Thermal radiation effects on the time-dependent MHD permeable flow having variable viscosity. Int J Thermal Sci 50(1):88–96
16. Turkyilmazoglu M (2012) Effects of uniform radial electric field on the MHD heat and fluid flow due to a rotating disk. Int J Eng Sci 51:233–240
17. Turkyilmazoglu M (2012) Three dimensional MHD stagnation flow due to a stretchable rotating disk. Int J Heat Mass Transfer 55(23–24):6959–6965
18. Turkyilmazoglu M (2012) MHD fluid flow and heat transfer with varying Prandtl numbers due to a rotating disk subject to a uniform radial electric field. Appl Thermal Eng 35:127–133
19. Asghar S, Jalil M, Hussan M, Turkyilmazoglu M (2014) Lie group analysis of flow and heat transfer over a stretching rotating disk. Int J Heat Mass Transfer 69:140–146
20. Makukula ZG, Sibanda P, Motsa SS (2012) On a quasilinearisation method for the von Karman flow problem with heat transfer. Latin American Appl Res 42(1):97–102
21. Arikoglu A, Komurgoz G, Ozkol I, Gunes AY (2010) Combined effects of temperature and velocity jump on the heat transfer, fluid flow, and entropy generation over a single rotating disk. Trans ASME J Heat Transfer 132(7). Paper 111703
22. Aly EH, Soliman HA (2011) Solution for steady flow over a rotating disk in porous media with heat transfer. J Appl Sci Res 7(11):1485–1491
23. Devi SPA, Devi RU (2011) On hydromagnetic flow due to a rotating disk with radiation effects. Nonlin Anal Model Control 16(1):17–29
24. Ariel PD (1996) The flow near a rotating disk: an approximate solution. Trans ASME J Appl Mech 63(2):436–438
25. Chen JX, Gan X, Owen JM (2001) Heat transfer from air-cooled contra-rotating disks. Trans ASME J Turbomach 119(1):61–67
26. Karabay H, Chen J-X, Pilbrow R, Wilson M, Owen JM (1999) Flow in a "cover-plate" preswirl rotor-stator system. Trans ASME J Turbomach 121(1):161–166
27. Karabay H, Wilson M, Owen JM (2001) Predictions of effect of swirl on flow and heat transfer in a rotating cavity. Int J Heat Fluid Flow 22:143–155
28. Kilic M, Owen JM (2003) Computation of flow between two disks rotating at different speeds. Trans ASME J Turbomach 125(2):394–400
29. Ong CL, Owen JM (1991) Computation of the flow and heat transfer due to a rotating disc. Int J Heat Fluid Flow 12(2):106–115
30. Oehlbeck DL, Erian FF (1979) Heat transfer from axisymmetric sources at the surface of a rotating disk. Int J Heat Mass Transfer 22(6):601–610
31. Pilbrow R, Karabay H, Wilson M, Owen JM (1999) Heat transfer in a 'cover-plate' pre-swirl rotating-disc system. Trans ASME J Turbomach 121(2):249–256
32. Prata AT, Pilichi CDM, Ferreira RTS (1995) Local heat transfer in axially feeding radial flow between parallel disks. Trans ASME J Heat Transfer 117(1):47–53
33. Roy RP, Xu G, Feng J (2001) A study of convective heat transfer in a model rotor-stator disk cavity. Trans ASME J Turbomach 123(3):621–632
34. Tadros SE, Erian FF (1983) Heat and momentum transfer in the turbulent boundary layer near a rotating disk. Paper ASME 83–WA/HT–6

35. Tadros SE, Erian FF (1982) Generalized laminar heat transfer from the surface of a rotating disk. Int J Heat Mass Transfer 25(11):1651–1660
36. Volkov KN, Hills NJ, Chew JW (2008) Simulation of turbulent flows in turbine blade passages and disc cavities. In: Proceedings of ASME Turbo Expo 2008, 4(Pts. A & B). Berlin, Germany, pp 1543–1554
37. Wu CM, Li YR, Ruan DF (2013) Aspect ratio and radius ratio dependence of flow pattern driven by differential rotation of a cylindrical pool and a disk on the free surface. Phys Fluids 25(8). Paper 084101
38. Yan Y, Gord MF, Lock GD, Owen JM (2003) Fluid dynamics of a pre-swirl rotor-stator system. Trans ASME J Turbomach 125(4):641–647
39. Cebeci T, Bradshaw P (1984) Physical and computational aspects of convective heat transfer. Springer, Berlin
40. Launder BE, Sharma BI (1974) Application of the energy dissipation model of turbulence to the calculation of the flow near a spinning disc. Lett Heat Mass Transfer 1:131–138
41. Morse AP (1988) Numerical prediction of turbulent flow in rotating cavities. Trans ASME J Turbomach 110(2):202–215
42. Morse AP (1991) Assessment of laminar-turbulent transition in closed disc geometries. Trans ASME J Turbomach 113(2):131–138
43. Derevich IV (2005) Modeling of the motion of particles in a rotary crusher. Theor Foundations Chem Eng 39(2):213–219
44. Lam CKG, Bremhorst KA (1981) Modified form of the k–ε model for predicting wall turbulence. Trans ASME J Fluid Eng 103(3):456–460
45. Arani AAA, Shahmohamadia P, Sheikhzadeha G, Mehrabianb MA (2013) Convective heat transfer from a heated rotating disk at arbitrary inclination angle in laminar flow. IJE Trans B Appl (Int J Eng) 26(8):865–874
46. Harmand S, Pellé J, Poncet S, Shevchuk IV (2013) Review of fluid flow and convective heat transfer within rotating disk cavities with impinging jet. Int J Thermal Sci 67:1–30
47. Indinger T, Shevchuk IV (2004) Transient laminar conjugate heat transfer of a rotating disk: theory and numerical simulations. Int J Heat Mass Transfer 47(14–16):3577–3581
48. Kumar BGV, Chew JW, Hills NJ (2013) Rotating flow and heat transfer in cylindrical cavities with radial Inflow. ASME J Eng Gas Turb Power 135(3). Paper 032502
49. Poncet S, Schiestel R (2007) Numerical modeling of heat transfer and fluid flow in rotor-stator cavities with throughflow. Int J Heat Mass Transfer 50:1528–1544
50. Poncet S, Nguyen TD, Harmand S, Pellé J, Da Soghe R, Bianchini C, Viazzo S (2013) Turbulent impinging jet flow into an unshrouded rotor–stator system: hydrodynamics and heat transfer. Int J Heat Fluid Flow 44:719–734
51. Roy KER, Prasad BVSSS, Murthy SS, Gupta NK (2005) Conjugate heat transfer in an arbitrary shaped cavity with a rotating disk. Heat Transfer Eng 25(8):69–79
52. Shevchuk IV, Delas NI (2005) Aerodynamics and turbulent flow heat exchange in the rotary disk air cleaner. Heat Transfer Res 36(1–2):104–113
53. Wu X, Squires KD (2000) Prediction and investigation of the turbulent flow over a rotating disk. J Fluid Mech 418:231–264
54. Helcig C, aus der Wiesche S (2013) The effect of the incidence angle on the flow over a rotating disk subjected to forced air streams. In: Proceedings of FEDSM 2013, Incline Village, Nevada, USA. Paper FEDSM2013-16360
55. Poncet S, Serre E (2009) High-order LES of turbulent heat transfer in a rotor-stator cavity. Int J Heat Fluid Flow 30(4):590–601
56. Tuliszka-Sznitko E, Zielinski A, Majchrowski W (2009) LES of the non-isothermal transitional flow in rotating cavity. Int J Heat Fluid Flow 30(3):543–548
57. aus der Wiesche S (2004) LES study of heat transfer augmentation and wake instabilities of a rotating disk in a planar stream of air. Heat Mass Transfer 40(3–4):271–284
58. aus der Wiesche S (2007) Heat transfer from a rotating disk in a parallel air crossflow. Int J Thermal Sci 46(8):745–754
59. Childs PRN (2011) Rotating flow. Elsevier Inc., Amsterdam

60. Loitsyanskii LG (1966) Mechanics of liquids and gases. Pergamon, Oxford
61. Shevchuk IV, Khalatov AA (1997) Integral method for calculating the characteristics of a turbulent boundary layer on a rotating disk: quadratic approximation of the tangent of the flow swirl angle. Heat Transfer Res 28(4–6):402–413
62. Baibikov AS (1998) Method of calculation of a turbulent flow in an axial gap with a variable radius between a rotating disk and an axisymmetric casing. J Eng Phys Thermophys 71(6):1072–1081
63. McComas ST, Hartnett JP (1970) Temperature profiles and heat transfer associated with a single disc rotating in still air. In: Proceedings of IV IHTC, Paris-Versailles, France, vol 3, Paper FC 7.7
64. Newman BG (1983) Flow and heat transfer on a disk rotating beneath a forced vortex. AIAA J 21(8):1066–1070
65. Cobb EC, Saunders OA (1956) Heat transfer from a rotating disk. Proc Roy Soc A 236:343–349
66. Kabkov VIa (1978) Heat transfer at air flow in a gap between a disk and a deflector rotating together with it. In: Teploobmen v Energeticheskikh Ustanovkakh, Naukova Dumka, Kiev, pp 121–124 (in Russian)
67. Mager A (1952) Generalization of boundary-layer momentum-integral equations to three-dimensional flows including those of rotating system. NACA Rep 1067:1–37
68. Shvets IT, Dyban EP (1974) Air cooling of gas turbine parts. Naukova Dumka, Kiev (in Russian)
69. Kabkov VIa (1974) Characteristics of turbulent boundary-layer on a smooth disk rotating in a large volume. Teplofizika i Teplotekhnika, Naukova Dumka, Kiev 28:119–124 (in Russian)
70. Littel HS, Eaton JK (1994) Turbulence characteristics of the boundary layer on a rotating disk. J Fluid Mech 266:175–207
71. Itoh M, Hasegawa I (1994) Turbulent boundary layer on a rotating disk in infinite quiescent fluid. JSME Int J Ser B 37(3):449–456
72. Elkins CJ, Eaton JK (1997) Heat transfer in the rotating disk boundary layer. Stanford University, Department of Mechanical Engineering, Thermosciences Division Report TSD–103. Stanford University (USA)
73. Cheng W-T, Lin H-T (1994) Unsteady and steady mass transfer by laminar forced flow against a rotating disk. Wärme und Stoffübertragung 30(2):101–108
74. Elkins CJ, Eaton JK (2000) Turbulent heat and momentum transfer on a rotating disk. J Fluid Mech 402:225–253
75. Case P (1966) Measurements of entrainment by a free rotating disk. J Roy Aero Soc 71:124–129
76. Abrahamson S, Lonnes S (1993) An integral method for turbulent boundary layers on rotating disks. Trans ASME J Fluids Eng 115(4):614–619
77. Abrahamson S, Lonnes S (1994) An improved model for radial injection between corotating disks. Trans ASME J Fluids Eng 116(2):255–257
78. Truckenbrodt E (1954) Die turbulente Strömung an einer angeblasenen rotierenden Scheibe. Z Angew Math Mech 34:150–162
79. Kapinos VM (1964) Heat transfer of a turbine rotor with a radial coolant flow. Inzhenerno-Fizicheskiy Zhurnal 7(1):3–11 (in Russian)
80. Kapinos VM (1965) Heat transfer from a disc rotating in a housing with a radial flow of coolant. J Eng Phys Thermophys 8(1):35–38
81. Kapinos VM (1965) Heat transfer of a disk rotating in a housing. Izvestiya vuzov. Aviatsyonnaya Tekhnika 2:76–86 (in Russian)
82. Goldstein S (1935) On the resistance to the rotation of a disc immersed in a fluid. Proc Cambridge Phil Soc 31:232–241
83. Johnson MC (1980) Turbulent heat transfer to a rotating disk: a review and extension of Dorfman. Trans ASME J Heat Transfer 102(4):780–781
84. Kapinos VM (1964) Hydraulic resistance and heat transfer of a free disc with a cob. Izvestiya vuzov Energetika 11:85–92 (in Russian)

85. Kapinos VM (1965) Effect of a radial gradient of a relative circumferential velocity component on heat transfer in forced flow between two rotating disks. Izvestiya vuzov Energetika 3:111–120 (in Russian)
86. Kapinos VM, Pustovalov VN, Rud'ko AP (1971) Heat transfer in a coolant flow from a center to a periphery between two rotating disks. Izvestiya vuzov Energetika 6:116–124 (in Russian)
87. Lokai VI, Bodunov MN, Zhuikov VV, Shchukin AV (1985) Heat transfer in cooled parts of aircraft gas-turbine engines. Izdatel'stvo Mashinostroenie, Moscow, USSR (in Russian)
88. Northrop A, Owen JM (1988) Heat transfer measurements in rotating-disc systems. Part 1: The free disc. Int J Heat Fluid Flow 9(1): 19–26
89. Northrop A (1984) Heat transfer in a cylindrical rotating cavity. D. Phil. thesis. University of Sussex, Brighton, UK
90. Kays WM, Crawford ME, Weigand B (2005) Convective heat and mass transfer, 4th edn. Mc-Graw-Hill, New York. ISBN:0-07-246876-9
91. Shevchuk IV, Khalatov AA (1997) The integral method of calculation of heat transfer in the turbulent boundary layer on a rotating disk: quadratic approximation of the tangent of the flow-swirl angle. Promyshlennaya Teplotekhnika 19(4–5):145–150 (in Russian)
92. Shevchuk IV (1998) Heat transfer in underswirled radial turbulent outflow in the gap between co-rotating discs of gas turbine rotors. Promyshlennaya Teplotekhnika 20(1):54–58 (in Russian)
93. Shevchuk IV (1998) Simulation of heat transfer in a rotating disk: the effect of approximation of the tangent of the angle of flow swirling. High Temp 36(3):522–524
94. Shevchuk IV, Khalatov AA, Karabay H, Owen JM (1998) Heat transfer in turbulent centrifugal flow between rotating discs with flow swirling at the inlet. Heat Transfer Res 29(6–8):383–390
95. Shevchuk IV (1998) The effect of distribution of radial velocity in the flow core on heat transfer under conditions of centrifugal flow in a gap between parallel rotating disks. High Temp 36(6):972–974
96. Shevchuk IV (1999) Integral method of calculation of a turbulent centrifugal underswirl flow in a gap between parallel rotating disks. Heat Transfer Res 30(4–6):238–248
97. Shevchuk IV (1999) Effect of wall-temperature distribution on heat transfer in centrifugal flow in the gap between parallel rotating disks. J Eng Phys Thermophys 72(5):896–899
98. Shevchuk IV (1999) Simulation of heat transfer and hydrodynamics over a free rotating disk using an improved radial velocity profile. J. Thermal Sci 8(4):243–249
99. Shevchuk IV (2000) Turbulent heat transfer of rotating disk at constant temperature or density of heat flux to the wall. High Temp 38(3):499–501
100. Shevchuk IV (2001) Effect of the wall temperature on laminar heat transfer in a rotating disk: an approximate analytical solution. High Temp 39(4):637–640
101. Shevchuk IV (2001) An improved enthalpy-thickness model for predicting heat transfer of a free rotating disk using an integral method. In: Proceedings of 35th ASME NHTC'01, Anaheim, California, USA. Paper NHTC2001–20195
102. Shevchuk IV, Saniei N, Yan XT (2001) Effect of the wall temperature distribution in direct and inverse problems of laminar heat transfer over a free rotating disk. In: Proceedings of 35th ASME NHTC'01, Anaheim, California, USA. Paper NHTC2001–20196
103. Shevchuk IV (2001) Turbulent heat transfer over a free rotating disk: analytical and numerical predictions using solutions of direct and inverse problems. In: Proceedings of IMECE'01, New York, USA, pp 1–8
104. Shevchuk IV (2002) Numerical modeling of turbulent heat transfer in a rotating disk at arbitrary distribution of the wall temperature. J Eng Phys Thermophys 75(4):885–888
105. Shevchuk IV, Saniei N, Yan XT (2002) Impinging jet heat transfer over a rotating disk: exact solution and experiments. In: Proceedings of 8th AIAA/ASME Joint Thermophys Heat Transfer Conference, St. Louis, Missouri, USA, Paper AIAA 2002–3015
106. Shevchuk IV, Saniei N, Yan XT (2003) Impingement heat transfer over a rotating disk: integral method. AIAA J Thermophys Heat Transfer 17(2):291–293

107. Shevchuk IV (2005) A new type of the boundary condition allowing analytical solution of the thermal boundary layer equation. Int J Thermal Sci 44(4):374–381
108. Shevchuk IV, Buschmann MH (2005) Rotating disk heat transfer in a fluid swirling as a forced vortex. Heat Mass Transfer 41(12):1112–1121
109. Shevchuk IV (2009) An integral method for turbulent heat and mass transfer over a rotating disk for the Prandtl and Schmidt numbers much larger than unity. Heat Mass Transfer 45 (10):1313–1321